

Development of an Efficient Numerical Simulation Method for Atmospheric and Hydrological Phenomena

Sumitomo Chemical Co., Ltd.
Production & Safety Fundamental Technology Center
Naoki SHIMADA



The following two numerical methods were developed in order to provide several computational methods that overcome the computing load issues of three-dimensional simulations based on fluid dynamics:

- (1) a method incorporating bent channel shapes in structured grids (improved cut-cell method)
- (2) a stable method for solving flows using a high aspect ratio grid

In the first method, we attempted to improve the cut-cell method for boundary layer computation near industrially important walls. The improvement demonstrated that the cavity flow and the flow around obstacles can be calculated accurately. In the second method, we confirmed that the same flow field can be calculated even when the aspect ratio of the computational grid is increased from 1 to 100, and we simulated the temperature and flow of a large-scale ocean area.

This paper is translated from R&D Report, "SUMITOMO KAGAKU", vol. 2021.

Introduction

In order to help establish a sustainable society, Sumitomo Chemical Co., Ltd. is making more strenuous efforts to promote the preservation of atmospheric and aquatic environments. To solve environmental issues, various specific innovations have to be propelled in accordance with the SBTs (science based targets)¹⁾.

Numerical simulation can be a powerful tool to evaluate environments. One of the most precise tools is CFD (computational fluid dynamics), which is a three-dimensional simulation method that provides quantitative evaluation taking into account complicated conditions such as geographical features, fluid discharge conditions, and multidimensional environmental fields. Meanwhile, one of the major issues is computer resources. Applying CFD is the mainstream method to solving discrete partial differential equations in three-dimensional spaces divided into computational grids or particles (elements which a space is broken down into). Therefore, the computational load strongly depends on the number of grids or cells. For

calculations in industrial apparatus scale, calculations use from 10^6 to 10^7 grids. The world-class record in 2020 used approximately an order of 10^{12} grids. Computers are being advanced rapidly today, and even greater performance is expected in the future. However, it will require a considerable amount of time and financial resources to become able to perform practical computations on an environmental scale (as large as kilometers). Therefore, commercial CFD software packages are thought to be impractical in many environmental simulation fields, in which models processed with statistical averages are usually used. Software packages such as TRACE²⁾, ALOHA³⁾, and METI-LIS⁴⁾ use diffusion models with coefficients that are adjusted for turbulent diffusion properties, which enables them to calculate fast. Because of this, they are used for risk screening. However, because processes using statistical means lose multidimensional geographical features and detailed input data, discussions on model verification will always be required.

The purpose of this paper is to provide some computational methods that overcome the computing load

issues of commercially available general CFD software packages. Specifically, the following two methods are provided:

- (1) a method incorporating bent channel shapes in structured grids (improved cut-cell method); and
- (2) a stable method for solving flows using a high aspect ratio grid.

Conventional flow simulation methods

Since 1913 when Prof. Richardson proposed the concept of numerical computation⁵⁾, CFD has been one of the challenging issues in computer simulation for more than one hundred years. Higher computing speed and precision, in particular, are important factors to be pursued. R&D efforts are continued today for overcoming these targets. First, many types of fluids are now calculated approximately as incompressible matter. This approximation assumes that density does not depend on pressure. Textbooks, handbooks, and software manuals describe that incompressible approximation can be allowed when the Mach number, M , is 0.3 or less. High-speed railways such as bullet trains are within this range, and many types of fluid simulations are conducted under incompressible approximation. However, it is not clearly explained why the criterion is 0.3. Part of Kajishima's lecture⁶⁾ is revised here to describe the grounds for this criterion. Assuming the use of an ideal gas, the following formulae will be obtained by applying the conservation of kinetic energy (Bernoulli equation) and the equation of state to a field of no velocity and a field of a flow with a velocity of v .

$$p_0 = p + \frac{1}{2} \rho v^2 \quad (1)$$

$$p_0 = \rho_0 RT \quad (2)$$

$$p = \rho RT \quad (3)$$

$$v = aM \quad (4)$$

Here, p_0 represents the stagnation pressure, p , the flow pressure, ρ , the flow density, ρ_0 , the stagnation density, R , the gas constant, T , the temperature, and a , the speed of sound. Assuming this is air at room temperature, the following equation is obtained after rearranging eqs. (1) to (4) in which $a \approx 340 \text{ m/s}$, $R \approx 286.7 \text{ J/(kg} \cdot \text{K)}$, and $T \approx 300\text{K}$.

$$\frac{\rho_0}{\rho} = 1 + 0.672M^2 \quad (5)$$

When $M = 0.3$, eq. (5) gives $\rho_0/\rho \approx 1.06$. This means that since the maximum change in density is approximately 6% at $M = 0.3$, the density can be approximated as constant. Incidentally, $M = 1$, which gives $\rho_0/\rho \approx 1.67$, does not allow for approximation of constant density. In chemical plants, changes in temperature and chemical reactions often have impacts on densities. In this case, there is a concern if the method of incompressibility approximation, which provides efficient computation, can be used. However, this issue has been overcome by past studies^{7), 8)}. For details, refer to the author's work.

The following Navier-Stokes equation is a basic equation for incompressible fluids.

$$\rho \left(\frac{\partial v}{\partial t} + v \cdot \nabla v \right) = -\nabla p + \nabla \tau \quad (6)$$

Here, v represents the velocity vector, t , the time, and τ , the stress tensor. The left side of the above equation expresses the change in velocity and the right side expresses the force taken into account. This can be interpreted as an equation of motion for a continuum system. Although the three-dimensional field with respect to v can be obtained from this equation, it has yet to be mathematically proven if a smooth solution exists. This is because it is an equation with properties of both hyperbolic and elliptic partial differential equations. In order to obtain a numerical approximate solution in the CFD, the Helmholtz-Hodge orthogonal decomposition theorem⁹⁾ is used. In other words, finding the appropriate orthogonal projection operators to separate vector fields, and then processing the equation by a two-step approach. For example, the fractional step method¹⁰⁾, the MAC method¹¹⁾, the SMAC method¹²⁾, and the SIMPLE method¹³⁾ have been developed.

Improvement of the cut-cell method

In the early stages of CFD research (until the 1960s), flow motions were calculated using regular grids or particles. Regularly arranged grids are called structured grids. After that, Steger *et al.* proposed the calculation of deformation grids based on coordinate transformation in 1978, and then in 1980s, finite element methods and finite volume methods were developed for unstructured grids. Because many industrial devices have complex shapes, unstructured grids, which are

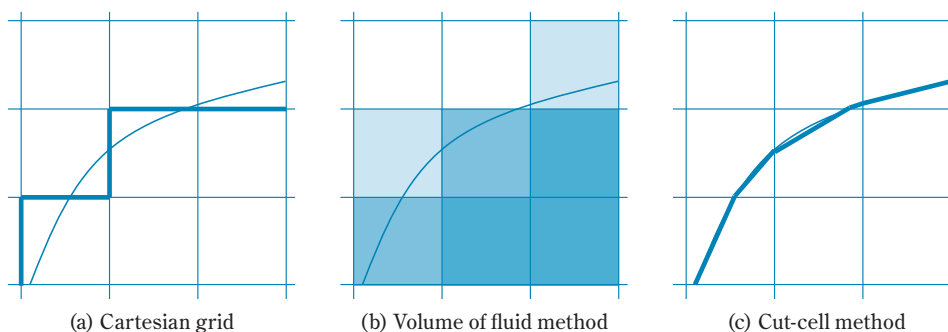


Fig. 1 Description of boundaries in the Cartesian grid²⁰⁾

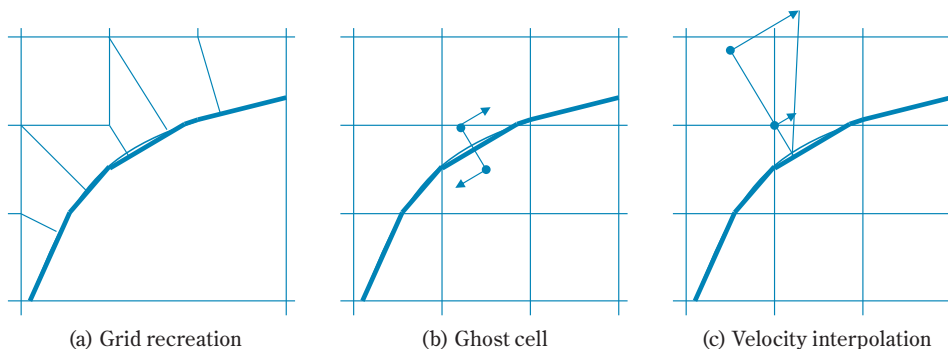


Fig. 2 Existing cut-cell methods²⁰⁾

geometrically flexible, became popular as a universal method. Today, many commercial software packages, such as ANSYS Fluent¹⁴⁾ and Siemens Star-ccm+¹⁵⁾, adopt unstructured grids. However, irregular arrangement of unstructured grids is likely to increase the computation time for data referencing and cause problems with spatial accuracy. For this reason, in the 21st century, there is a movement¹⁶⁾ to reexamine using structured grids as a method that can use and refer to the cache memory and main memory efficiently, and to easily increase spatial accuracy.

Fig. 1 shows some boundary representations using orthogonal structured grids. Method (a) is simple, but it cannot represent solid surfaces smoothly. Method (b) mitigates the problem of (a) by taking into consideration the occupied volume fraction of fluids or solids. However, it requires ingenuity to calculate the stress caused by the walls, and guaranteeing the rule of mass conservation may render the algorithm complex. In that respect, method (c), the cut-cell method, has advantages in that it can guarantee mass conservation and can easily simplify the algorithm. For this reason, we are focusing on the cut-cell method. The idea of cut-cell method itself has been pioneered by Clarke *et al.* (1986)¹⁷⁾, Tucker and Pan (2000)¹⁸⁾, and Ingram *et al.* (2003)¹⁹⁾.

In **Fig. 2**, existing cut-cell methods are categorized into three types. Method (a) is not substantially different from unstructured grids, and cannot exhibit the advantages of structured grids. Methods (b) and (c) arrange virtual points in the normal direction of boundaries to calculate velocities so that they may satisfy the boundary conditions. These methods place importance on the discussion for controlling flux along the boundary shape and they have not overcome the difficulty in dealing with wall friction. In other words, there remain challenging issues in the computation of boundary layers near industrially important walls. For this reason, we attempted to improve the cut-cell method²⁰⁾.

We replace equation (6) with the following integral type over range Ω .

$$\int_{\Omega} \rho \frac{\partial v}{\partial t} dV + \oint_{\partial\Omega} (\rho v v + p - \tau) \cdot n dA = 0 \quad (7)$$

Here, V represents the volume of the domain and A represents the area that encloses the domain. In the cut-cell method, we discuss how to deal with the second term of the left side of eq. (7). Here, the discussion is narrowed down to the accurate numerical handling of τ . For simplicity, the following explains a two-dimensional case. Parameter τ consists of the following four components:

$$\tau = \begin{pmatrix} \tau_{xx} & \tau_{xy} \\ \tau_{yx} & \tau_{yy} \end{pmatrix} \quad (8)$$

Let us consider an example in which the walls have impacts on τ_{yx} . We define a grid corresponding to i and j in the x and y directions, respectively, and then describe τ_{yx} on the upper right in **Fig. 3** as $\tau_{yx}(i+1/2, j+1/2)$. **Fig. 3** assumes that the rectangular grid at (i, j) includes wall surfaces and the wall is in contact with $(i, j-1/2)$. Let β_x represent the ratio of fluid at the right part of this grid. The geometrical relationship gives the following interpolation equations:

$$\tau_{yx}\left(i+\frac{1}{2}, j-\frac{1}{2}\right) = \frac{\tau_w/\cos\theta + \left(1-\beta_x\left(i+\frac{1}{2}, j\right)\right)\tau_{yx}\left(i+\frac{1}{2}, j+\frac{1}{2}\right)}{\beta_x\left(i+\frac{1}{2}, j\right)} \quad (9)$$

$$\theta = \left| \tan^{-1}\left(\beta_x\left(i-\frac{1}{2}, j\right) - \beta_x\left(i+\frac{1}{2}, j\right)\right) \right| \quad (10)$$

Given the friction τ_w on the wall, τ in the grid is obtained from eqs. (9) and (10), and then eq. (8) can be numerically calculated. The modelling of τ_w is one of the issues actively discussed in the CFD research

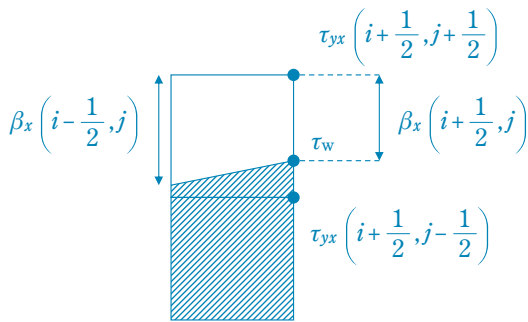
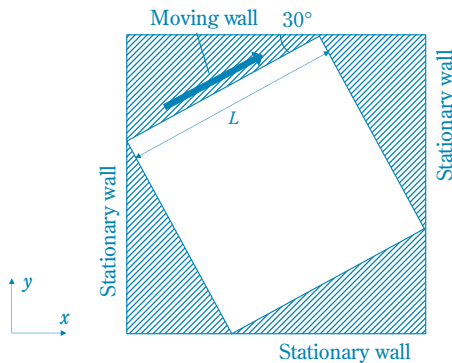
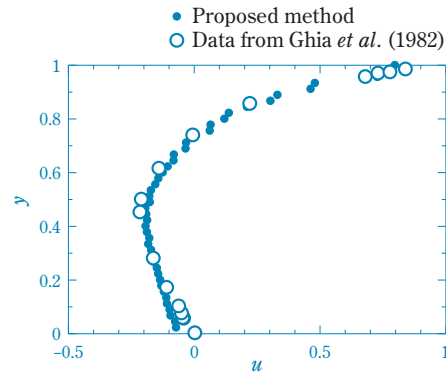


Fig. 3 τ at grid (i, j) ²⁰⁾



(a) Calculation domain



(b) Comparison of velocity profiles

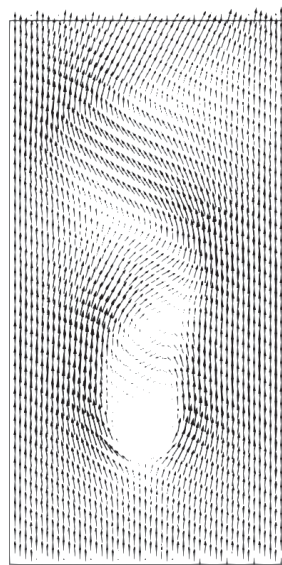
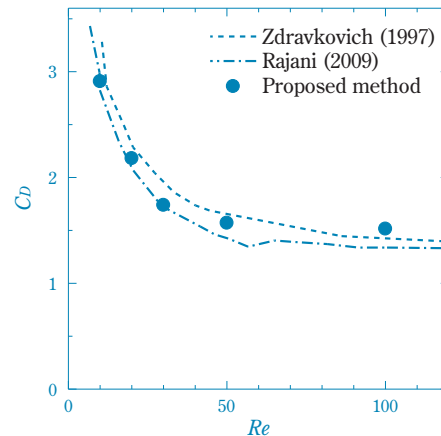
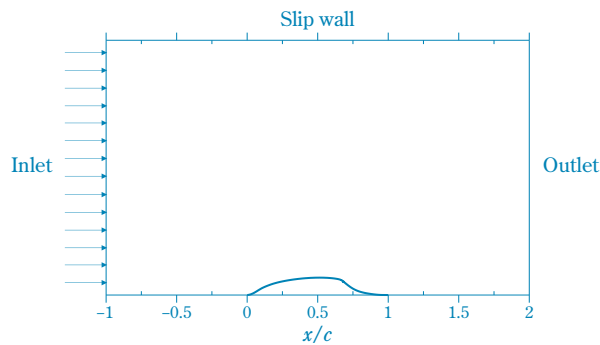
Fig. 4 Two-dimensional cavity flow with moving wall²⁰⁾

community. For example, the calculation of LES (large eddy simulation), which is one of the turbulence models, requires a large spatial resolution near walls to improve the accuracy, which in turn increases the number of grids. Meanwhile, the appropriate modelling of τ_w can suppress the increase in computing load. Balakumar *et al.* (2014)²¹⁾, Iyer and Malik (2016)²²⁾, Park and Moin (2016)²³⁾, and Berger and Aftosmis (2018)²⁴⁾ conducted WMLES (wall-modeled large eddy simulations) that combine τ_w modelling and LES, and verified that this combination is technically effective. However, Iyer and Malik's computation (2016) took about 11 days with 11 million grids and 320 parallel cores. The development of τ_w modelling was also advanced by Claft *et al.* (2002)²⁵⁾, Suga (2010)²⁶⁾, and Allmaras *et al.* (2012)²⁷⁾.

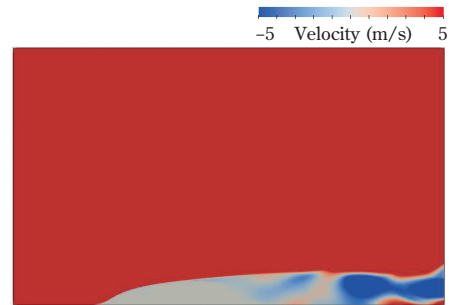
The newly developed method is known as the improved cut-cell method. Some computation examples by using the method are shown below:

(1) Two-dimensional inclined cavity flow

Fig. 4 shows an example of computing the flow inside a rectangular space inclined at 30 degrees with one moving wall. This is a popular simulation conducted by Ghia *et al.* (1982)²⁸⁾ and often referred to as a benchmark for flow computation. The moving wall gives frictional force τ_w to the fluid to induce a circulating flow inside the space. **Fig. 4(b)** shows the comparison results. The horizontal axis represents the flow velocity along the moving wall, and the vertical axis represents the computation position. Even though the wall is inclined at 30 degrees, these two simulation results are closely matched, demonstrating that our proposed method is effective.

(a) Velocity profile ($Re=100$)(b) Variation of mean C_D **Fig. 5** Three-dimensional flow around a cylinder²⁰⁾

(a) Calculation domain



(b) Velocity magnitude profiles

Fig. 6 Turbulent flow over wall-mounted hump²⁰⁾

(2) Flow around an object

Fig. 5 shows the computation results of flow around a three-dimensional cylinder. **Fig. 5(a)** shows the flow velocity distribution at a cylinder Reynolds number (Re) of 100. This shows a Kármán vortex is generated at the downstream side of the cylinder. **Fig. 5(b)** compares the time-averaged values of the drag coefficient (C_D) exerted on the cylinder. Our results match well with the data of Zdravkovich (1997)²⁹⁾ and Rajani (2009)³⁰⁾ for Re dependency of the mean C_D .

Fig. 6 shows the simulation of a turbulent flow over a wall-mounted hump. This is a comparative verification problem of turbulent models under the initiative of NASA (National Aeronautics and Space Administration, USA)³¹⁾. Greenblatt *et al.* (2006)³²⁾ performed experiments using this shape, and our data matched well for the time-averaged value of main flow velocity distribution.

Stable method for solving flows using high aspect ratio grids

In order to understand the environments of rivers, lakes, and oceans, water flow surveys are especially important. Since the 1980s, many flow simulations have been conducted (such as Blumberg and Mellor (1987)³³⁾, Mellor (1996)³⁴⁾, Hosoyamada *et al.* (1997)³⁵⁾, and Horiguchi *et al.* (2006)³⁶⁾). From the viewpoint of practical use, CFD has the following two problems:

- (1) In many cases, the vertical length scale is smaller than the horizontal one (*e.g.*, by an order of 1/1000 to 1/10)
- (2) The large impact of free surfaces

Due to problem (1), in particular, many simulations use hydrostatic pressure and shallow water flow approximations. In other words, several layers of horizontal two-dimensional domains are stacked in the vertical

direction in this approach, and completely coupled three-dimensional computations are not conducted. In order to overcome this issue, it is necessary to reconsider the method that handles the Navier-Stokes equation (6) numerically using high aspect ratio grids. For this reason, we reexamined the orthogonal decomposition theorem. The grid used for numerical computation refers to spatial widths that can decompose the field. In other words, a high aspect ratio means that this grid has different capture widths corresponding to different coordinate axes. Therefore, we decompose the vector field as follows.

$$v = \bar{v} + v' \tag{11}$$

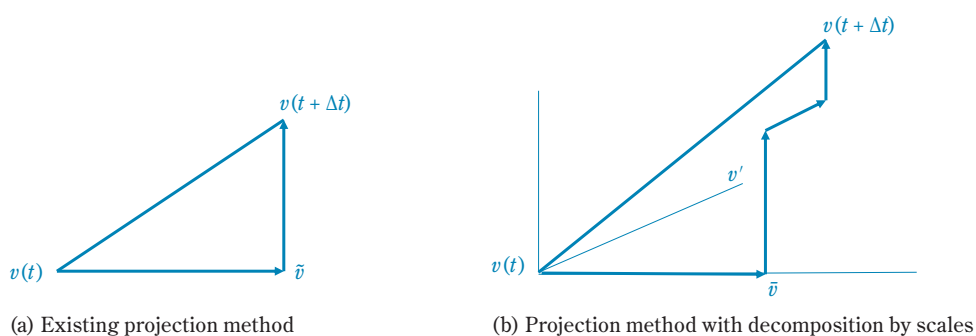


Fig. 7 Conceptual images of projection methods

Here, “ $\bar{\quad}$ ” denotes the longer size, and “ $'$ ” denotes the shorter size. **Fig. 7** shows conceptual images of the Helmholtz-Hodge orthogonal decomposition theorem. In obtaining the velocity field $v(t + \Delta t)$ at the point when Δt has passed after a time t , v travels via predictor \bar{v} according to the orthogonal decomposition theorem. Various types of operators (projection operators) to obtain \bar{v} have been proposed. In (b), the dimension to be projected is increased by one according to the size. In other words, the projection operator is further decomposed in accordance with the long and short sizes. For details on the decomposed formulae, refer to the author’s works^{37), 38)}.

Another numerical solution similar to this is the

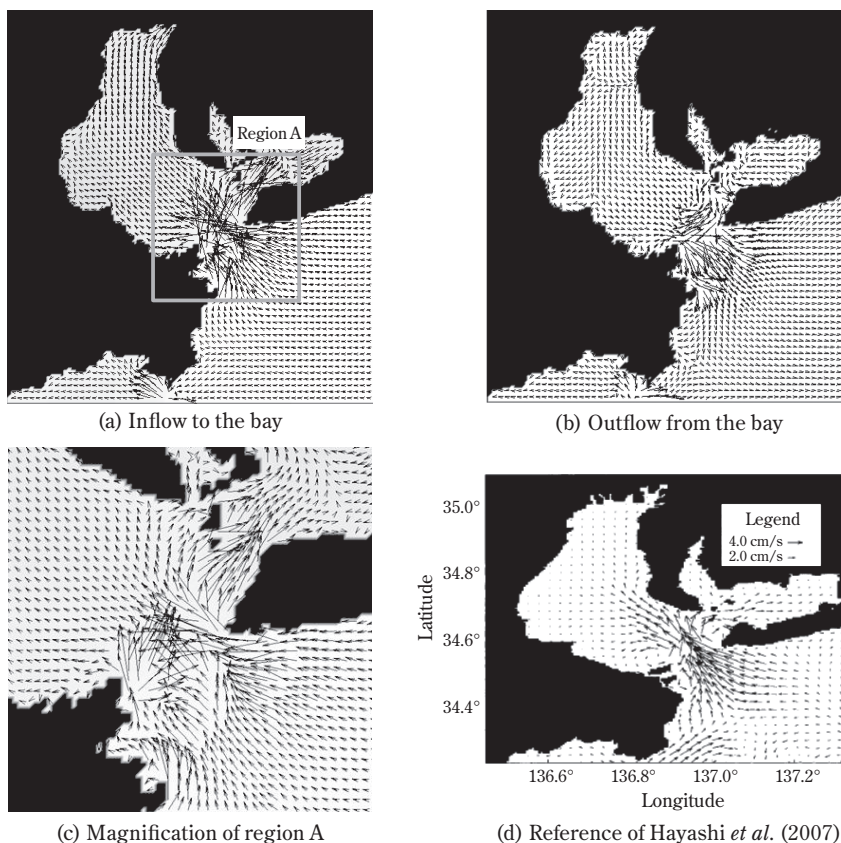


Fig. 8 Comparison of flow profiles³⁸⁾

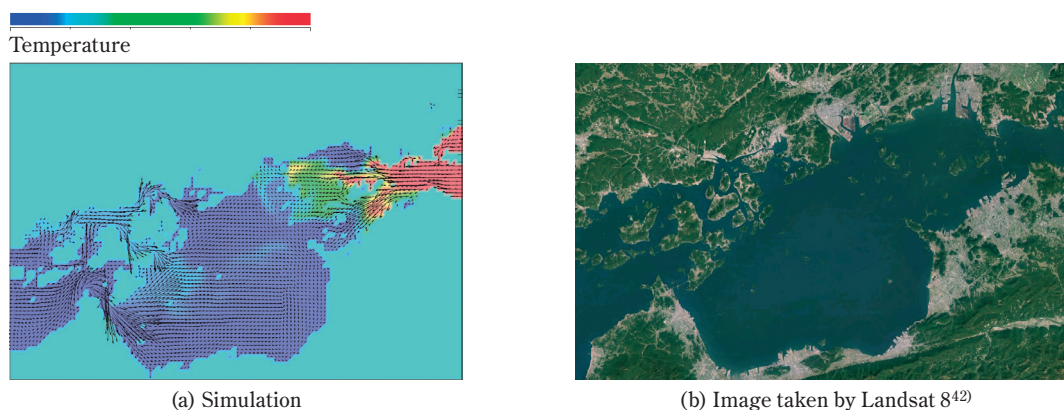


Fig. 9 Flow and temperature in Seto Inland Sea

multigrid method (Hackbusch, 1985)³⁹⁾ for computing the Poisson equation. However, many existing methods do not take into consideration coordinate components. We confirmed that, by our newly developed method, the same flow field can be calculated even when the aspect ratio of the computational grid is increased from 1 to 100.

Fig. 8 shows some computation examples using our developed method. Water depth data and observation data provided by the Japan Oceanographic Data Center⁴⁰⁾ were used as the input values. The computation data by Hayashi *et al.* (2007)⁴¹⁾ is also presented here for comparison. These data match well qualitatively for the acceleration patterns of the tidal current at the strait of the bay. The computational domain is $88.5 \times 96 \times 0.16$ km. This means the length in the horizontal direction is 600 times greater than the length in the vertical direction. If we try to decompose the vertical direction to take detailed computational grids, the number of computational grids in existing CFD methods grows to the order of 10^{10} , increasing the load. In this computation, we use grids with a horizontal length of 500 m and a vertical length of 5 m, which is achieved using our method that is good at a high aspect ratio. The number of computational grids was 997,500, and the PC (CPU: Intel Xeon E2-2687 W, 3.4 GHz; Memory: 32 GB) operated for about 48 hours to calculate the 70-hour transient phenomena.

Finally, Fig. 9 shows a simulation of temperature and flow in the Seto Inland Sea where Ehime Works is located. As can be seen from the satellite photograph (the Geographical Survey Institute⁴²⁾), the Seto Inland Sea is dotted with many islands, and it is famous for complex and strong tidal currents caused by the large rise and fall of the tide. The method described earlier

was used to perform large-scale computations of these tidal currents.

Conclusion

There is a movement^{43), 44)} to improve computation efficiency by 2021 by prompting the shift from CPU performance-dependent computing to heterogeneous computing, where the CPU and GPU work cooperatively. Thus, the development of hardware and software technologies to accelerate computing speed is becoming more and more active. Still, improvement of flow simulation is a challenging issue in the 21st century.

In addition, as Kajishima (2014)⁴⁵⁾ and Menter (2020)⁴⁶⁾ pointed out, it is not realistic to develop new technologies using CFD only. Simulation needs to be connected to real phenomena using data science and mathematical statistics in the future. To that end, faster CFD will become increasingly important. We hope our efforts, including those in this paper, will help advance these technologies.

Reference

- 1) Ministry of the Environment, SBT Gaiyou Shiryou [SBT Overview Material], https://www.env.go.jp/earth/ondanka/supply_chain/gvc/files/SBT_gaiyou_20210319.pdf (Ref. 2021/4/6)
- 2) Sumika Technical Information Service Inc., Bousai Kanri Shien [Disaster Prevention Management Support], <https://www.stis.co.jp/service/disaster.html> (Ref. 2021/4/12)
- 3) United States Environmental Protection Agency, ALOHA software, <https://www.epa.gov/comeo/aloha-software> (Ref. 2020/10/21).

- 4) Japan Environmental Management Association for Industry, METI-LIS Moderu Puroguramu [METI-LIS Model Program], <http://www.jemai.or.jp/tech/medi-lis/analysis.html> (Ref. 2020/10/21).
- 5) M. Hino, *Ryuutairikigaku* [Hydrodynamics], Asakura Publishing (1992).
- 6) The Japan Society of Mechanical Engineers, Computational Mechanics Engineers (Thermal hydraulics) Koushuukai [Workshop] (2004).
- 7) N. Shimada and A. Tomiyama, *Kagaku Kogaku Ronbunshuu* [Collection of Chemical Engineering Papers], 31(1), 15 (2005).
- 8) N. Shimada *et al.*, *Kagaku Kogaku Ronbunshuu* [Collection of Chemical Engineering Papers], 31(6), 377 (2005).
- 9) T. Tanahashi, *CFD Keisan Ryuutairikigaku* [CFD Calculation of Hydrodynamics], IPC, (1994), p. 633.
- 10) J. Kim and P. Moin, *J. Comput. Phys.*, 59, 308 (1985).
- 11) F. H. Harlow and J. E. Welch, *Phys. Fluids*, 8, 2182 (1965).
- 12) A. A. Amsden and Harlow, *J. Comput. Phys.*, 6, 322 (1970).
- 13) S. V. Patankar (Translated by Y. Mizutani, M. Katsuki), *Konpyuta ni yoru netsu idou to nagare no suuchi kaiseki* [Numerical Analysis of Heat Transfer and Flow by Computer], Morikita Publishing (1985).
- 14) ANSYS Fluent, <https://www.ansys.com/> (Ref. 2021/1/19).
- 15) Simcenter STAR-CCM+, <https://www.plm.automation.siemens.com/global/en/products/simcenter/STAR-CCM.html> (Ref. 2021/1/19).
- 16) Edited by T. Kobayashi, *Suuchi Ryutairikigaku Handobukku* [Handbook of Numerical Hydrodynamics], Maruzen Publishing (2003).
- 17) D. Clarke *et al.*, *AIAA Journal*, 24(3), 353 (1986).
- 18) P. G. Tucker and Z. Pan, *Appl. Math. Model.*, 24, 591 (2000).
- 19) D. M. Ingram *et al.*, *Mathematics and Computers in Simulation*, 61, 561 (2003).
- 20) S. Tanaka and N. Shimada, *J. of Chem. Eng. Japan*, 53(12), 747 (2020).
- 21) P. Balakumar *et al.*, “Proceedings of the 2014 Summer Program”, Center for Turbulence Research-Stanford Univ. (2014), p. 407–415.
- 22) P. S. Iyer and M. R. Malik, 46th AIAA Fluid Conf. AIAA-6016-3186 (2016).
- 23) G. I. Park and P. Moin, “Annual Research Briefs - 2016”, Center for Turbulence Research – Stanford Univ. (2016), p. 39–50.
- 24) M. J. Berger and M. J. Aftosmis, *AIAA*, 56(2), 445 (2018).
- 25) T. J. Craft *et al.*, 12th Int. Heat Transfer Conf. (2002).
- 26) K. Suga (Eds.: R. S. Amano and B. Sundén), “Computational Fluid Dynamics and Heat Transfer: Emerging Topics”, WIT Press (2010), p. 331.
- 27) S. R. Allmaras *et al.*, Seventh Int. Conf. on Comput. Fluid Dynamics, ICCFD7-1902 (2012).
- 28) U. K. Ghia *et al.*, *J. Comput. Phys.*, 48, 387 (1982).
- 29) M. M. Zdravkovich, “Flow Around Circular Cylinders”, Volume 1, Oxford Science Publications (1997).
- 30) B. N. Rajani *et al.*, *Appl. Math. Model.*, 33, 1228 (2009).
- 31) Turbulence Modeling Resource – NASA: website, <https://turbmodels.larc.nasa.gov/> (Ref. 2020/10/21).
- 32) D. Greenblatt *et al.*, *AIAA Journal*, 44(2), 263 (2006).
- 33) A. F. Blumberg and G. L. Mellor (Ed.: N. S. Heaps), “Three-Dimensional Coastal Ocean Models, Volume 4”, American Geophysical Union (1987), p. 1–16.
- 34) G. Mellor (Ed.: T. Ezer), “Proceedings from the Princeton Ocean Model (POM) Users Meeting”, Princeton University (1996), p. 8.
- 35) T. Hosoyamada *et al.*, *Kaigan Kougaku Ronbunshuu* [Collection of Coastal Engineering Papers], 44, 86 (1997).
- 36) F. Horiguchi *et al.*, *Estuar., Coast. Shelf Sci.*, 70(4), 589 (2006).
- 37) Sumitomo Chemical Co., Ltd., JP 6576303 B2 (2019).
- 38) S. Senda and N. Shimada, *J. of Chem. Eng. Japan*, 52(1), 41 (2019).
- 39) W. Hackbusch, “Multi-Grid Methods and Applications”, Springer (1985).
- 40) Japan Oceanographic Data Center, https://www.jodc.go.jp/jodcweb/index_j.html (Ref. 2021/4/12).
- 41) H. Hayashi *et al.*, *Kaigan Kaiyou Kenkyuu* [Oceanographic Research], 44(2), 177 (2007).
- 42) Geospatial Information Authority of Japan, <http://maps.gsi.go.jp/development/ichiran.html>, Data source: Landsat 8 images (GSI, TSIC, GEO, Grid/AIST), Landsat 8 images (courtesy of the U. S. Geological Survey), submarine topography

- (GEBCO) (Ref. 2017/5/17).
- 43) OneAPI Programming Model, <https://www.oneapi.com/> (Ref. 2021/1/19).
- 44) NVIDIA HPC Software Development Kit, <https://developer.nvidia.com/hpc-sdk> (Ref. 2021/1/19).
- 45) T. Kajishima, Gakujutsu no Doukou [Trends in Science], 19(10), 54 (2014).
- 46) F. Menter *et al.*, Appl. Sci., 11(6), 2459 (2021).

PROFILE



Naoki SHIMADA

Sumitomo Chemical Co., Ltd.
Production & Safety Fundamental Technology Center
Senior Researcher, Ph.D. (Engineering)